

## **Cardanol and bisphenol-F based benzoxazines with zirconium phosphate reinforced composites coating for protecting the mild steel surface from corrosion**

Latha Govindraj<sup>1#</sup>, Hariharan Arumugam<sup>1#</sup>, Balaji Krishnasamy<sup>1</sup>, Kumaravel Ammasai<sup>2</sup>, Alagar Muthukaruppan<sup>1\*</sup>

<sup>1</sup>Polymer Engineering Laboratory, PSG Institute of Technology and Applied Research, Neelambur, Coimbatore - 641 062, Tamil Nadu, India.

<sup>2</sup>Department of Chemistry, PSG Institute of Technology and Applied Research, Neelambur, Coimbatore - 641 062, Tamil Nadu, India.

\*Corresponding author: [muthukaruppanalagar@gmail.com](mailto:muthukaruppanalagar@gmail.com)

#Both authors contributed equally

### **Abstract**

The present work is to develop and characterise the benzoxazines from cardanol and bisphenol-F with imidazole core based amine in order to utilize them in the form of (50/50 wt%) blended composites coating for corrosion resistance application. The benzoxazine blends were reinforced with varying weight percentages of (0.5, 1, 1.5, 2.0 and 2.5 wt%) of 3-glycidoxypropyltrimethoxysilane (GPTMS) functionalized zirconium phosphate (ZrP) to obtain respective composites blended coatings. The thermal stability of composites were studied by thermogravimetric analysis (TGA). In order to ascertain their hydrophobic behaviour the water contact angle studies were carried out and the values obtained for 0.5, 1, 1.5, 2.0 and 2.5 wt% GPTMS functionalized ZrP reinforced (50/50 wt% of C-ima/BF-ima) benzoxazines blended composites are 114,116,117,119,120 and 123° respectively. The UV shielding behaviour of ZrP reinforced polybenzoxazine blended composites material was also studied by UV-Vis spectroscopic technique and the results obtained infer that these materials possess good UV shielding behaviour. ZrP reinforced benzoxazine blended composites were coated on the mild steel specimens and their corrosion resisting behaviour was studied. Results of Nyquist plot and Tafel plot, ascertain that among the coated specimens, the specimen coated with 2.5 wt% ZrP reinforced poly(C-ima/BF-ima) blended composites exhibits highest corrosion resisting efficiency.

**Keywords:** Cardanol, bisphenol-F, imidazole core based amine, thermal stability, flame retardant behaviour, zirconium phosphate, water contact angle, UV shielding, corrosion resistance.

## Introduction

The protection of metallic substrates against corrosion is an important issue for industrial and commercial points of view. One of the convenient methods of approach to minimize the damage due to corrosion is the use of corrosion inhibitors, which are normally either organic or inorganic based materials chemical used in very low amounts that efficiently slow down the rate of corrosion.<sup>[1-4]</sup> Inorganic corrosion inhibitors such as chromate, dichromate and nitrite based coatings were used for many years to protect mild steel from corrosion.<sup>[5-7]</sup> The bio-toxicity of these inhibitors especially, chromate, has limited its applications. Hence, the development of alternative non-toxic corrosion inhibitors containing hetero atoms like N, O and S atoms are warranted at present in order to replace toxic inorganic corrosion inhibitors.<sup>[8-10]</sup>

In this context, polymeric materials of both naturally occurring and synthetic materials are considered as perfect replacement of inorganic coating materials for corrosion application.<sup>[11-14]</sup> Polymers are obtained from monomers having group of atoms linked to each other in amount sufficient to provide a set of properties. The importance of polymers is principally due to its availability, processability and cost effectiveness, in addition to their inherent stability and multiple active adsorption centers. The extensively used both thermoplastic and thermosetting polymeric coating materials are epoxies, polyacrylates, polyesters, polyamides, polyimides, polyethers, polypropylene, polyurethanes, polyvinylchloride, polyvinylpyrrolidone, polyaniline and polybenzoxazines, etc.<sup>[15-28]</sup> Organic and inorganic additives can also be used to improve the mechanical, thermal, dielectric barrier, anti-microbial and other surface related properties of coatings.<sup>[29-32]</sup>

Polybenzoxazine matrices<sup>[20]</sup> obtained from bio-sources were considered as an eco-friendly protective coating materials and are used to protect mild steel surfaces from corrosion.<sup>[31,32]</sup> Polybenzoxazines possess easy processability, cures without release of any by-products, low shrinkage behavior, molecular flexibility, possess an excellent thermal stability, chemical resistance, mechanical properties and cost competitive. <sup>[20],[33,34]</sup> Comparatively little attention has been devoted to bio-based polybenzoxazine matrices as coating and composites.<sup>[35-41]</sup> In the recent past, researchers around the world have turned their focus on bio-based polybenzoxazines to assess their utility in the form of coatings, matrices and composites towards corrosion resistant applications. Cardanol based benzoxazines were found to possess good hydrophobic nature because of m-substituted long aliphatic chain in its molecular structure and in turn contributes to improve hydrophobic film forming behaviour and other characteristic properties required for coating applications.<sup>[42-46]</sup>

The incorporation of imidazole core into benzoxazine molecular structure is expected to impart the UV shielding and corrosion resistivity behaviour. The imidazole molecular moiety contributes to enhance the thermal stability of polybenzoxazines.<sup>[47]</sup> Further, the reinforcement of functionalized GPTMS-ZrP improves both physical and chemical properties of matrices.<sup>[48-50]</sup>

In the present work, an attempt has been made to prepare 50/50 wt% blend of C-ima and BF-ima benzoxazines from obtained from both sustainable natural cardanol and synthetic bisphenol-F precursors based on the results obtained from previous studies carried out. The different weight percentages (0.5, 1.0, 1.5, 2.0, and 2.5 wt%) of 3-glycidoxypropyltrimethoxysilane (GPTMS) functionalized zirconium phosphate (ZrP) were reinforced with 50/50 wt% of C-ima and BF-ima blended benzoxazines to obtain respective ZrP reinforced composites. Thermal stability, morphological behaviour and water contact angle were studied by modern analytical techniques. The varying weight percentages of GPTMS functionalized ZrP reinforced C-ima and BF-ima composite coatings were coated over conditioned mild steel specimens and their corrosion resisting behaviour was studied by different corrosion measurement techniques. Data obtained from different studies are correlated, discussed and reported.

## **Experimental**

### ***Materials***

Cardanol was obtained from Sathya cashew products, Chennai, India. Bisphenol-F was received from Anabond Limited, Chennai, India. Paraformaldehyde, tetrahydrofuran (THF) (99%), ethanol and methanol (99.8%), zirconylchloride, anhydrous sodium sulphate, hydrazine hydrate, ammonium acetate, acetic acid and ortho-phosphoric acid were obtained from Qualigens, India. (3-glycidyloxypropyl)trimethoxysilane (GPTMS), benzil and 4-nitro benzaldehyde were purchased from Sigma Aldrich, India. Ethyl acetate and sodium hydroxide were received from SRL, India.

### ***Synthesis of imidazole based nitro derivative (IMN)***

The 2,4,5-trisubstituted imidazole based nitro compound was prepared by Debus-Radziszewski imidazole synthesis. The mixture of benzil (0.1 mole), 4-nitrobenzaldehyde and ammonium acetate (0.4 mole) were taken in a round bottomed three necked flask in the presence of acetic acid medium. Then the mixture was subjected to a continuous stirring with refluxed condition until the completion of reaction. The progress of the reaction was monitored through thin layer chromatography (TLC). After the reaction was completed, the

reaction mixture was poured into ice cold water, filtered and washed twice with water then dried at 60°C for overnight to obtain the product (IMN).<sup>[48]</sup> (Scheme 1 and Figure S1).

#### ***Synthesis of imidazole based amine (IMA)***

The synthesised imidazole based nitro (IMN) compound was reduced using 10% palladium on activated carbon (10% Pd/C) dispersed in ethanol. The suspension solution was refluxed with required amount of hydrazine monohydrate which was added slowly into the mixture. After refluxing for 5 h the reaction mixture was filtered hot to remove Pd/C and the filtrate will be cooled to precipitate the pure amino derivative (IMA).<sup>[48]</sup> (Scheme 1 Figure S2).

#### ***Synthesis of mono functional benzoxazine (C-ima)***

The synthesis of cardanol based monofunctional benzoxazine using imidazole core mono amine (ima) is shown in Scheme 2. 0.2 mole of paraformaldehyde and 0.1 mole of cardanol were mixed under vigorous stirring then 0.1 mole imidazole core mono amine (ima) also added separately in the absence of any solvent and the temperature was raised slowly to 110 °C. The stirring was continued until the completion of the reaction monitored using TLC. Then, the resulted product was poured into 2N sodium hydroxide solution in order to remove an unreacted phenol and then extracted with chloroform solvent. The separated organic layer was dried over an anhydrous sodium sulphate and filtered. Finally the solvent was removed under reduced pressure to obtain the product (C-ima) (Figure S3).<sup>[48]</sup>

#### ***Synthesis of bi-functional benzoxazine (BF-ima)***

0.1 mole of bisphenol-F, 0.2 mole of IMA and 0.4 mole of paraformaldehyde were placed into a 250 ml three necked round bottomed flask equipped with magnetic stirrer, thermometer and reflux condenser. The reaction mixture was heated under stirring at 100 °C for 5 h. The obtained reaction product was diluted by the addition (Scheme 3) of ethyl acetate and thoroughly washed with distilled water using a separating funnel. Then the organic phase obtained was collected and dried with anhydrous sodium sulphate and filtered. The solvent left in the product was removed under vacuum to collect the product (BF-ima) (Figure S4).<sup>[48]</sup>

#### ***Preparation of zirconium phosphate (ZrP)***

One equivalent of zirconyl chloride ( $ZrOCl_2 \cdot 8H_2O$ ) was mixed with 10 equivalents volume of ortho phosphoric acid (12.0 M  $H_3PO_4$ ) and sealed into a Teflon-lined autoclave pressure vessel and heated at 200 °C for 24 h and then cooled. Once, the autoclave reached to room temperature, the resulted white precipitate of ZrP was separated by centrifugation and the precipitate obtained was repeatedly washed with deionized water for three times and filtered.

Then the sample was dried in an oven at 70°C for an overnight and ground into fine powder for further use.<sup>[45,46,49]</sup>

#### ***Preparation of silane functionalization of ZrP***

The silane coupling agent viz., (3-glycidyloxypropyl)trimethoxysilane (GPTMS) was used to functionalize ZrP to facilitate the formation of three dimensional cross-linked network structure with benzoxazine moiety during curing. 4 ml of silane derivative was mixed with 95% absolute ethanol and 5% deionized water and the resulting solution was sonicated for 15 min. The pH of the solvent was initially adjusted to 4.5 using acetic acid and subsequently sonicated for 60min. in order to ensure the complete hydrolysis of silane derivative (GPTMS). Then 10 g of synthesized ZrP was added and the resulting mixture was again sonicated for 2 h. Then the product obtained was refluxed for 24 h at 80 °C and centrifuged with the addition of water followed by ethanol and hexane. The ZrP functionalized with silane derivative was further dried in hot air oven at 100 °C in order to remove the moisture and labelled as functionalized ZrP (Scheme 4).

#### ***Preparation of the coatings***

The required numbers of uniform size mild steel (MS) plates having the size of 2 cm x 1 cm were first thoroughly polished using emery paper and cleaned using acetone solvent and dried. Then these plates were placed on the horizontal table. A certain volume of blend of reinforced composite coatings was dropped on the mild steel plate separately and it was dried at the room temperature for 5 h then the coated specimens were cured in an air oven at 200 °C for 3 h.

#### ***Preparation of poly(C-ima/BF-ima) matrix coated MS plate***

The blend of benzoxazine monomers C-ima 50 wt% and BF-ima 50 wt% were dissolved in THF solvent and subjected to overnight agitation. Then the resulted homogenous blend was coated on MS plate and left to evaporate slowly at 50°C for 1 h. Then the temperature was raised to 200 °C for 3 h (Scheme 5).

#### ***Preparation of ZrP reinforced poly(C-ima/BF-ima) composites coated MS plate***

0.5, 1.0, 1.5, 2.0 and 2.5 wt% of silane functionalized zirconium phosphate was added into the THF solution containing blend of benzoxazines respectively and subjected to overnight agitation. Then the resulted homogenous blend was transferred into the respective silane coated glass plates and left to evaporate slowly at 50°C for 8h. Subsequently cured at 200 °C for 3 h each until the formation of the light brown coloured thin composite films (Scheme 6).

### **Characterization**

FTIR spectra measurements were carried out with Agilent Cary 630 FTIR Spectrometer. <sup>1</sup>H-NMR spectra were obtained with Bruker (400 MHz) using dimethylsulfoxide (d<sub>6</sub>-DMSO) as a solvent and tetramethylsilane (TMS) as an internal standard. DSC measurements were recorded using NETZSCH STA 449F3 under N<sub>2</sub> purge (60 mLmin<sup>-1</sup>) at scanning rate of 10°C min<sup>-1</sup>. Thermogravimetric analysis (TGA) was carried out from room temperature to 850°C using NETZSCH STA 449F3 with 5 mg of sample under N<sub>2</sub> flow (60 mL min<sup>-1</sup>) at heating rate of 20°C min<sup>-1</sup>. The morphology of the blended matrices and composites were analysed from an FEI QUANTA 200F high-resolution scanning electron microscope (HRSEM). Contact angle measurements were obtained using a Kyowa goniometer with 5µl of water as probe liquid. The benzoxazines coated mild steel plates were tested for their corrosion protection behavior on mild steel in 3.5% sodium chloride solution. The corrosion experiments on mild steel specimens were carried out using open-circuit potential (OCP), electrochemical impedance spectroscopy (EIS) and potentiodynamic polarisation. UV shielding of behaviour of benzoxazine blended composites coating materials was studied by JASCO UV DRS V-750, USA.

### **Results and discussion**

Cardanol and bisphenol-F based benzoxazines were prepared by Mannich condensation reaction separately with imidazole core amine and para-formaldehyde as shown in Schemes 1 and 2 respectively. After appropriate work-up, the obtained products of benzoxazines were isolated and characterized. The detailed molecular structure characterization and curing behaviour of benzoxazines were discussed in our previous work.<sup>[48]</sup> Based on the results obtained from previous work, 50 wt% of C-ima and 50 wt% BF-ima blend was prepared and studied in the present work. In the present study, it was observed that polybenzoxazines and ZrP reinforced blended benzoxazine composites possess better hydrophobic nature, due to the presence of side alkyl chain and heterocyclic core in their chemical structure. Further, it was also observed that the results obtained for polybenzoxazines blended composites possess an improved thermal stability, water repellency, better corrosion resistant properties and UV shielding behaviour (**Figure 1**).<sup>[50]</sup>

The molecular structure of synthesized benzoxazine monomers (C-ima and BF-ima) were ascertained using FTIR spectral studies (Figure S5). The appearance of bands at 1215 cm<sup>-1</sup> and 1088 cm<sup>-1</sup> correspond to C-O-C asymmetric stretching and symmetric stretching respectively and 916 cm<sup>-1</sup> represents C-H group (out of plane), which confirms the presence of benzene ring attached to a heterocyclic moiety. Similarly, the appearance of

absorption band at  $1514\text{ cm}^{-1}$  corresponds to aromatic in-plane vibration of disubstituted benzene, which also confirms the formation of benzoxazine monomers. The presence of C=N in the imidazole ring was also confirmed through the appearance of band at  $1600\text{ cm}^{-1}$ . [38] The  $^1\text{H-NMR}$  spectral studies also supports the proposed benzoxazine structure; it shows two typical singlet signals respectively at around 5.5 ppm represents (O-CH<sub>2</sub>-N) hydrogen atoms of the nitrogen and oxygen bonded methylene groups and around 4.8 ppm (Ar-CH<sub>2</sub>-N) represents hydrogen atoms of the nitrogen and aryl bonded methylene groups. [48]

The FTIR spectra of the synthesised ZrP and GPTMS functionalised F-ZrP are presented in Figure S6. For the ZrP spectrum, the peak at  $1250\text{ cm}^{-1}$  belongs to the out-of-plane bending vibration of P-OH. The strong absorption peak appeared at  $1029\text{ cm}^{-1}$  is the stretching vibration peak of -PO<sub>4</sub> group. The FTIR spectra of prepared ZrP are consistent with that of the standard ZrP FTIR spectra reported [39]. For the GPTMS functionalised ZrP spectra. The strong characteristic peaks which emerge near  $3000\text{--}2850\text{ cm}^{-1}$  are symmetrical and asymmetric stretching vibration peaks of methylene. Si-C characteristic absorption peaks are observed at  $1253\text{ cm}^{-1}$ . The oxirane ring stretching vibration is merged with ZrP belonging peaks at  $\sim 950\text{ cm}^{-1}$ , also a new band appeared near  $1730\text{ cm}^{-1}$  for C=O stretching that could be associated with the cleavage of the epoxide ring. The peak observed at  $1155\text{ cm}^{-1}$  confirms the presence of P-O-Si in the sample. Compared with the ZrP infrared spectra, these newly emerged peaks indicate that the GPTMS molecules are successfully attached to the ZrP crystal surface. The GPTMS does not insert into the ZrP crystal layer which still maintains a stable layered structure, and it only modifies the surface and the edge of the crystal (Figure S6).

Further, polymerisation process of benzoxazines proceeds with the ring opening of benzoxazine monomer and polymerization behavior of C-ima and BF-ima monomers were studied through DSC analysis at the heating rate of  $10^\circ\text{C min}^{-1}$  under nitrogen atmosphere. The curing of C-ima monofunctional benzoxazine monomer was observed at  $218^\circ\text{C}$ , whereas, that of BF-ima bifunctional benzoxazine monomer cures at  $202^\circ\text{C}$ . The thermal polymerization ( $T_p$ ) behavior of C-ima and BF-ima benzoxazine blends with 50/50 wt% was also observed through DSC analysis. The exothermic peaks (polymerization temperature,  $T_p$ ) observed in DSC thermograms for the blend such as C-ima/BF-ima is appeared at  $202^\circ\text{C}$ . Further, the curing of blends were also ascertained from the FTIR analysis, the absence of bands at  $1215\text{ cm}^{-1}$ ,  $1088\text{ cm}^{-1}$  and  $929\text{ cm}^{-1}$  after curing confirm the occurrence of ring opening reaction of blended benzoxazine monomers. The reactive methylene group abstracts



an ortho hydrogen present in the neighbouring oxazine ring and initiates the polymerization reaction (Figure S7 and S8).<sup>[40][20]</sup>

### ***Thermal behavior***

The thermal properties of cured benzoxazines and blends of poly(C-ima) and poly(BF-ima) were studied using TGA analysis under an inert condition and the data obtained are presented in Table 1. There was no weight loss observed below 150 °C which suggests that there are no volatiles and moisture present in the samples. The decomposition maxima ( $T_{max}$ ) for poly(C-ima), poly(BF-ima) and poly(50 wt% C-ima / 50 wt% BF-ima) were observed at 453, 491 and 468 °C, respectively. The residual char yield obtained at 850 °C for poly(C-ima), poly(BF-ima) and poly(50 wt% C-ima / 50 wt% BF-ima) are 23%, 61% and 45% respectively.

The thermal stability of polybenzoxazine and its composites were also studied using TGA at the heating rate of 20 °C per minute in nitrogen atmosphere and the results obtained are presented in Figure 2 and Table 2. It was noticed that the thermal degradation temperature and percentage char yield of 0.5, 1.0, 1.5, 2.0 and 2.5 wt% ZrP reinforced polybenzoxazines blended composites are increased with increasing the weight percentage of silane functionalized ZrP. This may be explained due to the retardation effect of heat transfer and thereby contributes to an enhanced thermal stability to the hybrid blend of ZrP reinforced nanocomposites. The presence of heterocyclic imidazole core also contributes to higher thermal stability, which in turn facilitates the higher volume of char upon heating. Further, the presence of ZrP retards the decomposition of carbonaceous mass, which in-turn results high residual mass of carbon and ZrP even at high temperature.

### ***Flame Retardant behavior***

The flame retardant behavior of the materials can be ascertained from the value of limiting oxygen index (LOI) calculated using char yield obtained from thermogravimetric analysis. The value of LOI is calculated using van Krevelen and Hoftyzer relation.<sup>[51-53]</sup>  $LOI = 17.5 + 0.4 CR$ . The percentage char yield (CR) of the sample obtained from TGA analysis at 850 °C is presented in Table 2. It is well known that the polymeric materials with LOI values greater than 26 possess flame retardant behaviour and are considered for flame retardant applications. The LOI value of blend of poly(C-ima / BF-ima) possesses a high char yield value of 44%. The polybenzoxazines blended composites offer the higher char residue and thereby enhances the value of LOI. The value of LOI increases with increase in ZrP content and it was observed that 2.5 wt% of ZrP reinforced composites possesses the highest



LOI value of 37.9. The results obtained in the present study are higher when compared with those reported earlier for cardanol-based benzoxazines.<sup>[41]</sup>

### ***Morphological studies***

The surface behaviour of the ZrP and DGEBA functionalised ZrP were studied with SEM images (Figure 3). Neat poly(C-ima / BF-ima) blended matrix, 0.5 wt%, 1 wt%, 1.5 wt% and 2.5 wt% ZrP reinforced poly(C-ima / BF-ima) composites were taken for SEM analysis and the results obtained are presented in Figure 4. ZrP reinforced benzoxazine matrices exhibit a homogenous morphology without any cracking and voids. During the increase of concentration of ZrP in benzoxazine hybrid composites, the rigidity of the benzoxazine composites also increased, which has proved by fractured structure of composites. ZrP reinforcement influences the formation of covalent bonds with benzoxazine matrices and led to occur the inter-cross linked network, which in-turn contributes to develop smooth surfaces. The data obtained from SEM studies infer that there was an effective formation of hybrid network structure between the components of blended benzoxazine matrix and silane functionalized ZrP.

### ***Contact angle***

The value of water contact angle and images of neat blend of poly(C-ima / BF-ima), 0.5 wt %, 1.0 wt % 1.5 wt%, 2.0 wt % and 2.5 wt % ZrP reinforced poly(C-ima / BF-ima) blended hybrid composites are given in Figure 5. The values of water contact angle obtained for 0.5, 1, 1.5, 2.0 and 2.5 wt% GPTMS functionalized ZrP reinforced (50 wt% / 50 wt% of C-ima / BF-ima) benzoxazines blended composites are 114, 116, 117, 119, 120 and 123° respectively. It is inferred from the values of water contact angle that all the samples exhibit hydrophobic behaviour and this may be explained due to the presence of the long aliphatic chain of cardanol moiety and nitrogen rich imidazole core. In addition, the intra-molecular hydrogen bonding results in enhanced water contact angle. Consequently, the developed polybenzoxazine composite matrix possesses a reduced surface free energy and enhanced hydrophobic behaviour suggest that these materials can be used as an effective insulation material under humid environments.

### ***Corrosion studies***

The measurement of corrosion protecting efficiency of the mild steel specimens were carried out using open-circuit potential (OCP), electrochemical impedance spectroscopy and potentiodynamic polarisation. The varying weight percentages (0.5, 1, 1.5, 2.0 and 2.5 wt%) of silane functionalized ZrP reinforced polybenzoxazine blended composites were used for

protection of surfaces of mild steel (MS) from corrosion. Results obtained from corrosion studies infer that the blend of polybenzoxazines reinforced with 2.5 wt% silane functionalized ZrP coated on mild steel specimen possess the higher protection than that of other wt% of ZrP reinforced composites coated mild steel specimens due to improved hydrophobic behaviour.

#### ***Corrosion studies using OCP measurements***

The plot is drawn between the open circuit potential (OCP) values and the time of immersion and is presented in Figure 6. From the Figure 6, it is ascertained that the OCP values of the coated specimens are shifted significantly to the anodic direction when compared with that of bare mild steel specimen. It can also be seen that the OCP values of ZrP reinforced poly(C-ima / BF-ima) composites coated specimens are decreased much slower rate when compared to that of the bare mild steel specimen. The increase in values of OCP shift toward positive direction indicated that the high corrosion resistance offered by the blend of benzoxazine coatings.<sup>[57-59]</sup> Among the GPTMS functionalized ZrP reinforced poly(C-ima/BF-ima) composites (0.5-2.5 wt%) coated specimens studied, poly(C-ima / BF-ima) with 2.5 wt% ZrP offers higher anodic shift of OCP values which indicates that this composite coatings form highly impervious and strong adherent film formed on the surface which in-turn prevents the permeability of the corrosion medium.<sup>[52,60]</sup>

Nyquist plots derived from the EIS measurements for benzoxazines blended coating samples with varying weight percentages (0.5, 1, 1.5, 2.0 and 2.5) of ZrP and uncoated mild steel specimens after immersion in 3.5% NaCl solution for 5 days are presented in Figure 7 and Table 3. The uncoated mild steel (MS) specimen exhibits a small capacitive loop indicating that the poor corrosion resistance. The ZrP reinforced benzoxazines blended hybrid coating specimens offer a single capacitive loop. The fitting of all EIS data was done using the equivalent circuit model (Figure 8).

This equivalent circuit is used to evaluate the data, where  $R_s$  is the solution resistance of the solution between the working electrode and the counter electrode.  $R_s$  values are not only depending on the ionic conductivity of the solution but also depending on the geometrical area of the electrode.  $R_s$  values are not an important data while studying the corrosion resisting behaviour of the film because it does not yield any information about the coatings.  $R_{ct}$  is the charge transfer resistance which are used to measure the resistance of the electron transfer across the metal-solution interface, which is inversely proportional to the corrosion rate of the metal.  $Q_c$  is the double layer capacitance,  $R_c$  is the coating resistance and  $C_{dl}$  is the coating capacitance. The calculated values of the corrosion parameters from EIS

measurements are presented in Table 3.  $R_{ct}$  values of the ZrP incorporated polybenzoxazines blended coated specimens are higher than that of the bare mild steel (MS) specimen. Corrosion resistance is also increased when ZrP concentration in the coating system was increased in the benzoxazines blended composites. The maximum  $R_c$  and  $R_{ct}$  values are obtained for the composites coating with 2.5 wt% ZrP coated on mild steel specimen. The improved corrosion resisting behaviour may be due to the reduction of pores/cavities present in the polymer coating which could be occupied by ZrP.<sup>[61-64]</sup> The roughness factor values ( $n$ ) are continuously decreasing while increasing the weight percentage of ZrP into the benzoxazines blended composites, which also corroborates the reduction of pores/cavities in the coated films on the steel surface. It is well known that, all the organic coatings are not completely impenetrable for long time, their barrier properties could decrease when immersion time increases because of the water/corrosion medium penetration into the coatings. For bare mild steel (MS) specimen, the corrosion medium had a direct contact with the metal surface which led to the generation of many electro-active sites and corrosion will take place freely. Actually, corrosion reaction will take place in the presence of moisture and oxygen. ZrP containing polymer coatings prevent the diffusion of oxygen because of the polymer matrix with three dimensional cross-linked network structure with ZrP reinforcement. From the contact angle measurement, it can also be understood that, all the ZrP containing coatings are hydrophobic in nature, which could effectively reduce the wettability of benzoxazines blended coatings, which ultimately reduces the sorption of water molecules on the coatings. Among the varying weight percentages of ZrP reinforced polybenzoxazine hybrid coatings used in the work, polybenzoxazine hybrid coating matrix with 2.5 wt% ZrP offers a better corrosion resistance behaviour than other wt% concentration of ZrP which is due to the efficient interaction occurred between the coating and the metal surface which in turn forms a strong binding film on the metal surface.

Figure 9 and Table 4, presents the Tafel plots of ZrP reinforced poly(C-ima/BF-ima) coated MS specimens. The corrosion rate (CR) was calculated using  $I_{corr}$  values with the help of the following equation,

$$CR = MI_{corr} / \rho nF$$

Where  $M$  is the molecular mass of copper ( $58.69 \text{ g mole}^{-1}$ ),  $I_{corr}$  is the corrosion current density ( $\text{A cm}^{-2}$ ),  $F$  is the Faradays constant ( $96500 \text{ A s mole}^{-1}$ ),  $\rho$  is the density of the mild steel specimen ( $7.85 \text{ g cm}^{-3}$ ), and the number of electrons transferred during corrosion reaction is assumed to be 2.<sup>[59]</sup>

The  $E_{\text{corr}}$  values of the ZrP reinforced polybenzoxazine coated MS specimens shifted anodically. The more anodic shift was observed for ZrP reinforced polybenzoxazine coated specimens. Maximum anodic shift was observed for polybenzoxazine coated mild steel specimen with 2.5 wt% ZrP. The  $I_{\text{corr}}$  values of ZrP reinforced polybenzoxazine coated specimens are also reduced indicating that the corrosion resistance of the coated specimens were improved after coating. These values corroborate the results observed from the EIS studies. The improved corrosion resistance arises from reinforcement of GPTMS functionalized ZrP and in-turn suppressed the anodic corrosion reactions.<sup>[60]</sup> The polybenzoxazine blended matrix reinforced with 2.5 wt% ZrP coating shows better corrosion resistant behaviour than that of other samples of polybenzoxazines blend with different wt% of ZrP. Comparatively the prepared benzoxazine composites have better corrosion resistant behaviour than other benzoxazine coatings.<sup>[49]</sup>

#### ***UV shielding ability of composites***

The transmission spectra in the UV–Vis region (200–850 nm) for neat poly(C-ima/BF-ima) matrix and poly(C-ima/BF-ima) blends with 0.5, 1.0, 1.5, 2.0 and 2.5 wt% of ZrP are presented in Figure 10. The transmittance of the composites is strongly decreased as the content of the silane functionalized ZrP increased. From these results (Figure 10), it is evident that the presence of even a small percentage incorporation of ZrP influences to an appreciable extent of UV shielding behaviour, which can be attributed either to the obtained structural phase or to the presence of distributed reinforcement ZrP. However, the poly(C-ima /BF-ima) blended matrix also contributes to the significant percentage reduction of transmittance in the visible range due to their inherent chemical nature.<sup>[50]</sup>

#### **Conclusion**

The varying weight percentages (0.5, 1, 1.5, 2.0 and 2.5 wt%) of functionalised ZrP was reinforced with blended 50/50wt% of benzoxazine (C-ima and BF-ima) monomers to obtain benzoxazine composite hybrid coatings. Thermal stability, morphology, UV shielding and water contact angle behaviour were studied using modern analytical techniques. Data obtained from thermal studies infer that these materials possess an excellent thermal stability with good flame retardancy. Results obtained from UV shielding studies infer that the ZrP reinforced polybenzoxazines possess good UV shielding behaviour according to the wt% of ZrP. Water contact angle studies ascertain that both the benzoxazine matrix and ZrP reinforced composite coatings exhibit hydrophobic character. Results from corrosion studies, showed that both the neat blended benzoxazine matrix and ZrP reinforced benzoxazine composite coatings exhibit good corrosion resisting behaviour according to the weight

percentage incorporation of ZrP reinforcement. However, among the coated specimens studied, the specimen coated with 2.5 wt% ZrP reinforced poly(C-ima/BF-ima) exhibits the highest corrosion resisting efficiency due to its formation of efficient adherent film and consequent water repellent character. Imidazole core benzoxazine also helps to improve the corrosion resistant and hydrophobic behaviors. Furthermore, ZrP reinforced nitrogen rich benzoxazine matrix also contributes to improve the flame retardant behavior.

Data resulted from different studies, it is concluded that the ZrP reinforced polybenzoxazine composite hybrid coatings can be used as a cost competitive and sustainable bio-composite hybrid coatings for the protection of mild steel surfaces from corrosion under adverse environmental conditions.

### **Acknowledgment**

The authors thank the PSG Management, Secretary, Principal, PSG Institute of Technology and Applied Research, Coimbatore-641062, India for their moral and financial support.

### **Conflict of interest**

The authors declare no conflict of interest.

### **References**

- [1] ArunKumar, S.; Jegathish, V.; Soundharya, R.; JesyAlka, M.; Arul, C.; Sathyanarayanan, S.; Mayavan, S. Evaluating the performance of MoS<sub>2</sub> based materials for corrosion protection of mild steel in an aggressive chloride environment. *RSC Adv.* **2017**, 7 (28), 17332–17335. doi:10.1039/c7ra01372h
- [2] Barroso, G.; Li, Q.; Bordia, R. K.; Motz, G. Polymeric and ceramic silicon-based coatings-a review. *J. Mater. Chem. A* **2019**, 7 (5), 1936–1963. doi:10.1039/c8ta09054h
- [3] Wei, H.; Wang, Y.; Guo, J.; Shen, N. Z.; Jiang, D.; Zhang, X.; Yan, X.; Zhu, J.; Wang, Q.; Shao, L.; Lin, H.; Wei, S.; Guo, Z. Advanced micro/nanocapsules for self-healing smart anticorrosion coatings. *J. Mater. Chem. A* **2015**, 3 (2), 469–480. doi:10.1039/c4ta04791e
- [4] Ates, M. A review on conducting polymer coatings for corrosion protection. *J. Adhes. Sci. Technol.* **2016**, 30 (14), 1510–1536. doi:10.1080/01694243.2016.1150662
- [5] Roetheli, B. E.; Cox, G. L. Prevention of Corrosion of Metals by Sodium Dichromate as Affected by Salt Concentrations and Temperature. *Ind. Eng. Chem.* **1931**, 23 (10), 1084–1090. doi:10.1021/ie50262a002
- [6] Taylor, S. R. Coatings for Corrosion Protection: Inorganic. *Encycl. Mater. Sci. Technol.* **2001**, 1263–1269. doi:10.1016/b0-08-043152-6/00238-2
- [7] Hayyan, M.; Sameh, S. A.; Hayyan, A.; AlNashef, I. M. Utilizing of sodium nitrite as

- inhibitor for protection of carbon steel in salt solution. *Int. J. Electrochem. Sci.* **2012**, *7* (8), 6941–6950
- [8] Singh, A.; Talha, M.; Xu, X.; Sun, Z.; Lin, Y. Heterocyclic Corrosion Inhibitors for J55 Steel in a Sweet Corrosive Medium. *ACS Omega* **2017**, *2* (11), 8177–8186. doi:10.1021/acsomega.7b01376
- [9] Singh, A.; Ansari, K. R.; Quraishi, M. A.; Kaya, S.; Banerjee, P. The effect of an N-heterocyclic compound on corrosion inhibition of J55 steel in sweet corrosive medium. *New J. Chem.* **2019**, *43* (16), 6303–6313. doi:10.1039/c9nj00356h
- [10] Ahmed, S. K.; Ali, W. B.; Khadom, A. A. Synthesis and investigations of heterocyclic compounds as corrosion inhibitors for mild steel in hydrochloric acid. *Int. J. Ind. Chem.* **2019**, *10* (2), 159–173. doi:10.1007/s40090-019-0181-8
- [11] Mardare, L.; Benea, L. Development of Anticorrosive Polymer Nanocomposite Coating for Corrosion Protection in Marine Environment. *IOP Conf. Ser. Mater. Sci. Eng.* **2017**, *209* (1). doi:10.1088/1757-899X/209/1/012056
- [12] Al-Shahrani, A.; Taie, I.; Fihri, A.; Alabedi, G. Polymer-Clay Nanocomposites for Corrosion Protection. *Curr. Top. Util. Clay Ind. Med. Appl.* **2018**. doi:10.5772/intechopen.74154
- [13] Xu, H.; Zhang, Y. A Review on Conducting Polymers and Nanopolymer Composite Coatings for Steel Corrosion Protection. *Coatings* **2019**, *9* (12), 807. doi:10.3390/coatings9120807
- [14] Zhang, J.; Huang, H.; Ma, J.; Huang, L.; Huang, L.; Chen, X.; Zeng, H.; Ma, S. Preparation and Properties of Corrosion-Resistant Coatings From Waterborne Polyurethane Modified Epoxy Emulsion. *Front. Mater.* **2019**, *6* (August), 1–9. doi:10.3389/fmats.2019.00185
- [15] Hsissou, R.; Dagdag, O.; Berradi, M.; El Bouchti, M.; Assouag, M.; Elharfi, A. Development rheological and anti-corrosion property of epoxy polymer and its composite. *Heliyon* **2019**, *5* (11), 1–10. doi:10.1016/j.heliyon.2019.e02789
- [16] Ruhi, G.; Dhawan, S. K. Conducting Polymer Nano Composite Epoxy Coatings for Anticorrosive Applications. *Mod. Electrochem. Methods Nano, Surf. Corros. Sci.* **2014**. doi:10.5772/58388
- [17] Lakshmikandhan, T.; Hariharan, A.; Sethuraman, K.; Alagar, M. Development of functionalized SiO<sub>2</sub>–TiO<sub>2</sub> reinforced cardanol and caprolactam modified diamine based polybenzoxazine nanocomposites for high performance applications. *J. Coatings Technol. Res.* **2019**, *16* (6), 1737–1749. doi:10.1007/s11998-019-00263-w

- [18] Selvaraj, V.; Raghavarshini, T. R. Building up of Prosopis juliflora carbon incorporated cardanol based polybenzoxazine composites with intensification of mechanical and corrosion resistance properties for adaptable applications. *Polym. Bull.* **2019**, No. 0123456789. doi:10.1007/s00289-019-03084-4
- [19] Zhang, R.; Lu, X.; Lou, C.; Zhou, C.; Xin, Z. Preparation of diamine-based polybenzoxazine coating for corrosion protection on mild steel. *J. Polym. Res.* **2019**, *26* (2). doi:10.1007/s10965-018-1683-3
- [20] Zhang, S.; Yin, S.; Ran, Q.; Fu, Q.; Gu, Y. Facile preparation of polybenzoxazine/graphene nanocomposites for electromagnetic interference shielding. *Polymer (Guildf)*. **2019**, *162*, 20–28. doi:10.1016/j.polymer.2018.12.024
- [21] Ghosh, N. N.; Kiskan, B.; Yagci, Y. Polybenzoxazines-New high performance thermosetting resins: Synthesis and properties. *Prog. Polym. Sci.* **2007**, *32* (11), 1344–1391. doi:10.1016/j.progpolymsci.2007.07.002
- [22] Hariharan, A.; Kesava, M.; Alagar, M.; Dinakaran, K.; Subramanian, K. Optical, electrochemical, and thermal behavior of polybenzoxazine copolymers incorporated with tetraphenylimidazole and diphenylquinoline. *Polym. Adv. Technol.* **2018**, *29* (1), 355–363. doi:10.1002/pat.4122
- [23] Dogan, Y. E.; Satilmis, B.; Uyar, T. Synthesis and characterization of bio-based benzoxazines derived from thymol. *J. Appl. Polym. Sci.* **2018**, *47371*, 1–10. doi:10.1002/app.47371
- [24] Calò, E.; Maffezzoli, A.; Mele, G.; Martina, F.; Mazzetto, S. E.; Tarzia, A.; Stifani, C. Synthesis of a novel cardanol-based benzoxazine monomer and environmentally sustainable production of polymers and bio-composites. *Green Chem.* **2007**. doi:10.1039/b617180j
- [25] Shukla, S.; Mahata, A.; Pathak, B.; Lochab, B. Cardanol benzoxazines-interplay of oxazine functionality (mono to tetra) and properties. *RSC Adv.* **2015**, *5* (95), 78071–78080. doi:10.1039/c5ra14214h
- [26] Arumugam, H.; Krishnan, S.; Chavali, M.; Muthukaruppan, A. Cardanol based benzoxazine blends and bio-silica reinforced composites: Thermal and dielectric properties. *New J. Chem.* **2018**, *42* (6), 4067–4080. doi:10.1039/c7nj04506a
- [27] Lochab, B.; Varma, I. K.; Bijwe, J. Cardanol-based bisbenzoxazines: Effect of structure on thermal behaviour. *J. Therm. Anal. Calorim.* **2012**, *107* (2), 661–668. doi:10.1007/s10973-011-1854-5
- [28] Hariharan, A.; Prabhunatha, P.; Manoj, M.; Alagar, M. Studies on heterocyclic amines



- based cardanol-benzoxazine for oil-water separation. *Polym. Engg. Sci.* **2020**, 60 (7), 1–13. doi:10.1002/pen.25396
- [29] Muthukaruppan, A.; Arumugam, H.; Krishnan, S.; Kannan, K.; Chavali, M. A low cure thermo active polymerization of chalcone based benzoxazine and cross linkable olefin blends. *J. Polym. Res.* **2018**, 25 (8) 163-174. doi:10.1007/s10965-018-1556-9
- [30] Shukla, S.; Yadav, N.; Lochab, B. Cardanol-Based Benzoxazines and Their Applications; Elsevier Inc., 2017. doi:10.1016/B978-0-12-804170-3.00024-X
- [31] Hariharan, A.; Prabunathan, P.; Subramanian, S. S.; Kumaravel, M.; Alagar, M. Blends of Chalcone Benzoxazine and Bio-benzoxazines Coated Cotton Fabrics for Oil–Water Separation and Bio-silica Reinforced Nanocomposites for Low-k Applications. *J. Polym. Environ.* **2019**, No. 0123456789. doi:10.1007/s10924-019-01629-2
- [32] Li, S.; Zhao, C.; Gou, H.; Li, Y.; He, X.; Zhao, L. Advanced anticorrosion coatings prepared from Polybenzoxazine/ $\alpha$ -zirconium phosphate nanocomposites. *Int. J. Electrochem. Sci.* **2018**, 13 (3), 2661–2675. doi:10.20964/2018.03.76
- [33] Xiao, Y.; Xu, J.; Huang, S.; Deng, H. Effects of  $\alpha$ -ZrP on Crystallinity and Flame-Retardant Behaviors of PA6/MCA Composites. *Int. J. Polym. Sci.* **2017**, 2017. doi:10.1155/2017/6034741
- [34] Zhao, C.; Li, P.; He, D.; Li, Y.; Lei, F.; Sue, H. J. Flame retardation behavior of polybenzoxazine/ $\alpha$ -ZrP nanocomposites. *RSC Adv.* **2016**, 6 (77), 73485–73495. doi:10.1039/c6ra18450b
- [35] Latha, G.; Hariharan, A.; Prabunathan, P.; Alagar, M. Cardanol-Imidazole Based Benzoxazine Blends and Bio-silica Reinforced Composites with Enhanced Surface, Thermal and Dielectric Properties. *J. Polym. Environ.* **2020**, 28 (3), 918–933. doi:10.1007/s10924-019-01649-y
- [36] Huang, T. C.; Lai, G. H.; Li, C. E.; Tsai, M. H.; Wan, P. Y.; Chung, Y. H.; Lin, M. H. Advanced anti-corrosion coatings prepared from  $\alpha$ -zirconium phosphate/polyurethane nanocomposites. *RSC Adv.* **2017**, 7 (16), 9908–9913. doi:10.1039/c6ra27588e
- [37] Prabunathan, P.; Thennarasu, P.; Song, J. K.; Alagar, M. Achieving low dielectric, surface free energy and UV shielding green nanocomposites: Via reinforcing bio-silica aerogel with polybenzoxazine. *New J. Chem.* **2017**. doi:10.1039/c7nj00138j
- [38] Zhang, S.; Ran, Q.; Fu, Q.; Gu, Y. Preparation of Transparent and Flexible Shape Memory Polybenzoxazine Film through Chemical Structure Manipulation and Hydrogen Bonding Control. *Macromolecules* **2018**, 51 (17), 6561–6570.

doi:10.1021/acs.macromol.8b01671

- [39] Han, L.; Chen, Q.; Chen, H.; Yu, S.; Xiao, L.; Ye, Z. Synthesis and performance of functionalized  $\alpha$ -zirconium phosphate modified with octadecyl isocyanate. *J. Nanomater.* **2018**, *2018*, 1-9. doi:10.1155/2018/5873871
- [40] Zhang, S.; Ran, Q.; Gu, Y. Polymerization mechanism of 1,3-benzoxazine catalyzed by  $\text{PCl}_5$  and rearrangement of chemical structures. *Eur. Polym. J.* **2021**, *142*, 110133. doi:10.1016/j.eurpolymj.2020.110133
- [41] Appavoo, D.; Amarnath, N.; Lochab, B. Cardanol and Eugenol Sourced Sustainable Non-halogen Flame Retardants for Enhanced Stability of Renewable Polybenzoxazines. *Front. Chem.* **2020**, *8*, 1–15. doi:10.3389/fchem.2020.00711
- [42] Khodair, Z. T.; Khadom, A. A.; Jasim, H. A. Corrosion protection of mild steel in different aqueous media via epoxy/nanomaterial coating: Preparation, characterization and mathematical views. *J. Mater. Res. Technol.* **2019**, *8* (1), 424–435. doi:10.1016/j.jmrt.2018.03.003
- [43] Arora, S.; Srivastava, C. Microstructure and corrosion properties of NiCo-graphene oxide composite coatings. *Thin Solid Films* **2019**, *677*, 45–54. doi:10.1016/j.tsf.2019.03.011
- [44] Hung, H. M.; Linh, D. K.; Chinh, N. T.; Duc, L. M.; Trung, V. Q. Improvement of the corrosion protection of polypyrrole coating for CT3 mild steel with 10-camphorsulfonic acid and molybdate as inhibitor dopants. *Prog. Org. Coatings* **2019**, *131*, 407–416. doi:10.1016/j.porgcoat.2019.03.006
- [45] Zhou, C.; Lu, X.; Xin, Z.; Liu, J.; Zhang, Y. Polybenzoxazine/SiO<sub>2</sub> nanocomposite coatings for corrosion protection of mild steel. *Corros. Sci.* **2014**, *80*, 269–275. doi:10.1016/j.corsci.2013.11.042
- [46] Bandeira, R. M.; van Drunen, J.; Tremiliosi-Filho, G.; dos Santos, J. R.; de Matos, J. M. E. Polyaniline/polyvinyl chloride blended coatings for the corrosion protection of carbon steel. *Prog. Org. Coatings* **2017**, *106*, 50–59. doi:10.1016/j.porgcoat.2017.02.009
- [47] Zhou, C.; Xin, Z. Polybenzoxazine-Based Coatings for Corrosion Protection; Elsevier Inc., **2017**. doi:10.1016/B978-0-12-804170-3.00046-9
- [48] Derradji, M.; Ramdani, N.; Zhang, T.; Wang, J.; Gong, L. D.; Xu, X. D.; Lin, Z. W.; Henniche, A.; Rahoma, H. K. S.; Liu, W. Bin. Effect of silane surface modified titania nanoparticles on the thermal, mechanical, and corrosion protective properties of a bisphenol-A based phthalonitrile resin. *Prog. Org. Coatings* **2016**, *90*, 34–43.

doi:10.1016/j.porgcoat.2015.09.021

- [49] Manoj, M.; Kumaravel, A.; Mangalam, R.; Prabunathan, P.; Hariharan, A.; Alagar, M. Exploration of high corrosion resistance property of less hazardous pyrazolidine-based benzoxazines in comparison with bisphenol-F derivatives. *J. Coatings Technol. Res.* **2020**. doi:10.1007/s11998-019-00312-4

DRAFT

## Scheme Captions

Scheme 1. Synthesis of 2,4,5-trisubstituted imidazole based amine (IMA) derivative

Scheme 2. Synthesis of C-ima benzoxazine monomer

Scheme 3. Synthesis of BF-ima benzoxazine monomer

Scheme 4. Preparation of Silane Functionalization of ZrP

Scheme 5. Synthesis of poly(C-ima/BF-ima) benzoxazines blended matrix

Scheme 6. Preparation of ZrP reinforced poly(C-ima/BF-ima) benzoxazines blended composites

## Figure Captions

**Figure 1. Benzoxazine coating on MS plate for hydrophobic, flame retardant and corrosion protection application.**

Figure 2. TGA thermogram of ZrP reinforced polybenzoxazine blended composites

**Figure 3. SEM micrographs of (a) ZrP, (b) GPTMS functionalised ZrP.**

Figure 4. SEM micrographs of (a) neat blend of poly(C-ima/BF-ima), (b) 0.5 wt %, (c) 1.0 wt % (d) 1.5 wt%, (e) 2.0 wt % and (f) 2.5 wt % ZrP reinforced poly(C-ima/BF-ima) blended composites

**Figure 5. The water contact angle of (a) neat blend of poly(C-ima/BF-ima), (b) 0.5 wt %, (c) 1.0 wt % (d) 1.5 wt%, (e) 2.0 wt % and (f) 2.5 wt % ZrP reinforced poly(C-ima/BF-ima) blended composites.**

Figure 6. Plot of  $E_{ocp}$  Vs time in 3.5% of NaCl solution for (a) bare mild steel specimen (b) neat matrix, (c) 0.5 wt%, (d) 1.0 wt%, (e) 1.5 wt%, (f) 2.0 wt% and (g) 2.5 wt% ZrP reinforced poly(C-ima/BF-ima)

Figure 7. EIS response of bare MS and ZrP reinforced poly(C-ima/BF-ima) benzoxazine blended composites coated specimen in 3.5% NaCl solution

Figure 8. The equivalent circuit used for impedance analysis

Figure 9. Tafel plots of bare MS and ZrP reinforced polymer composites coated specimens in 3.5% NaCl solution

Figure 10. UV transmittance spectra of neat poly(C-ima/BF-ima) matrix and ZrP reinforced poly(C-ima/BF-ima) composites

**Table Captions**

Table 1. Thermal behavior of neat benzoxazines matrices

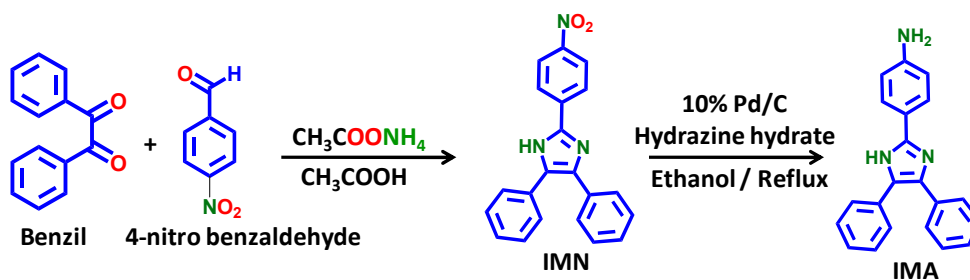
Table 2. Thermal properties and water contact angle values of ZrP reinforced polybenzoxazine blended composites

Table 3. Corrosion parameters of the coated and bare mild steel specimens in 3.5 % NaCl solution calculated from potentiodynamic polarisation studies

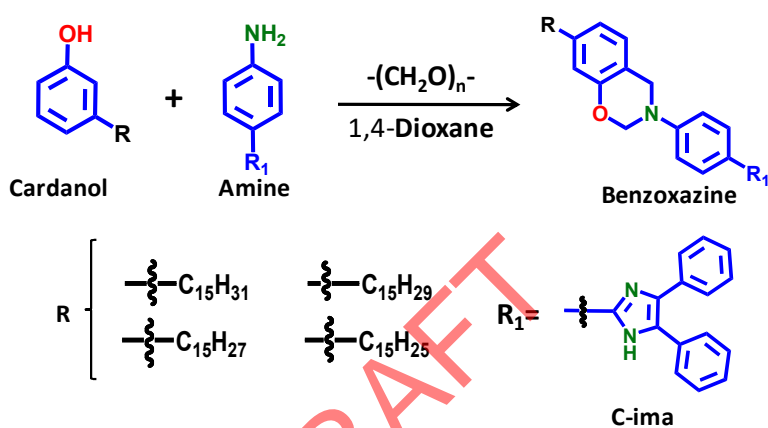
Table 4. The values of the corrosion parameters of the coated and uncoated mild steel specimens in 3.5 % NaCl solution calculated from Tafel studies

DRAFT

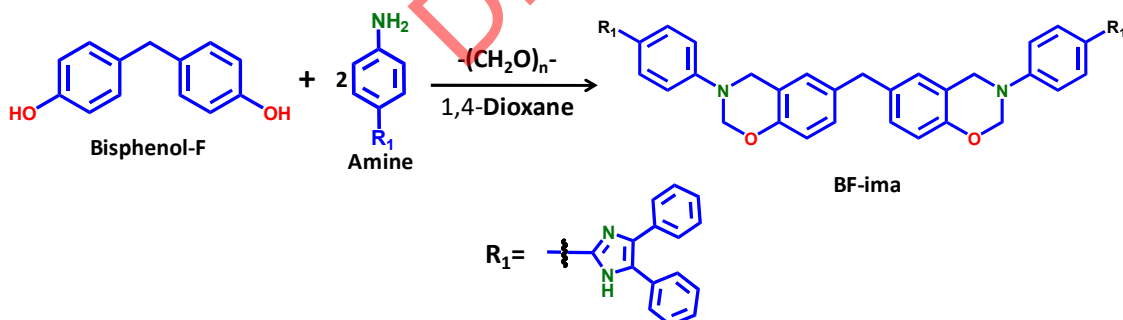
## Schemes and Figures



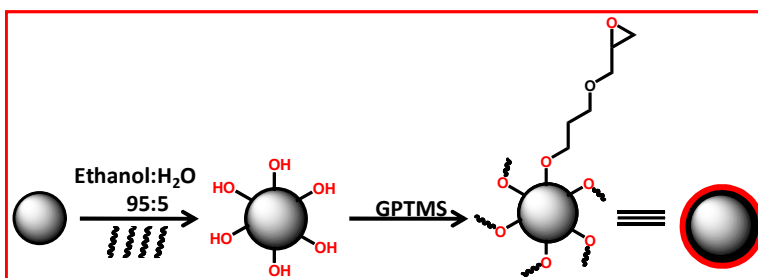
Scheme 1. Synthesis of 2,4,5-trisubstituted imidazole based amine (IMA) derivative



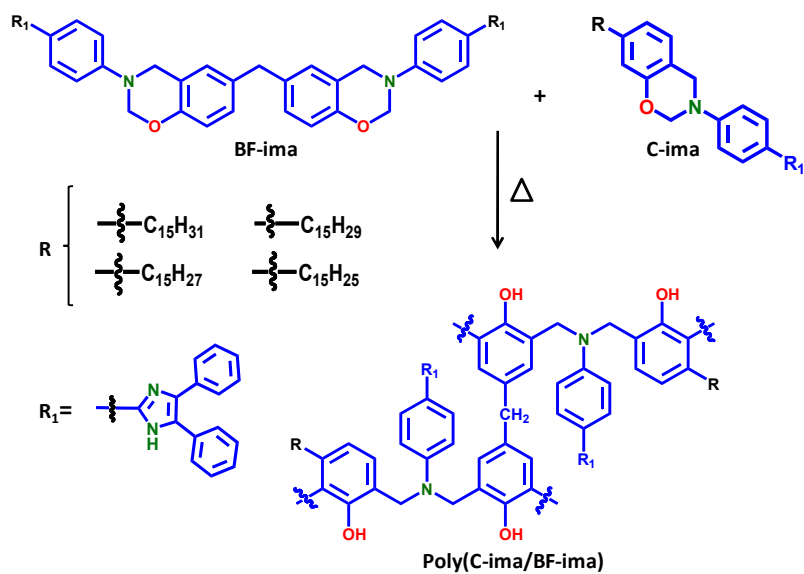
Scheme 2. Synthesis of C-ima benzoxazine monomer



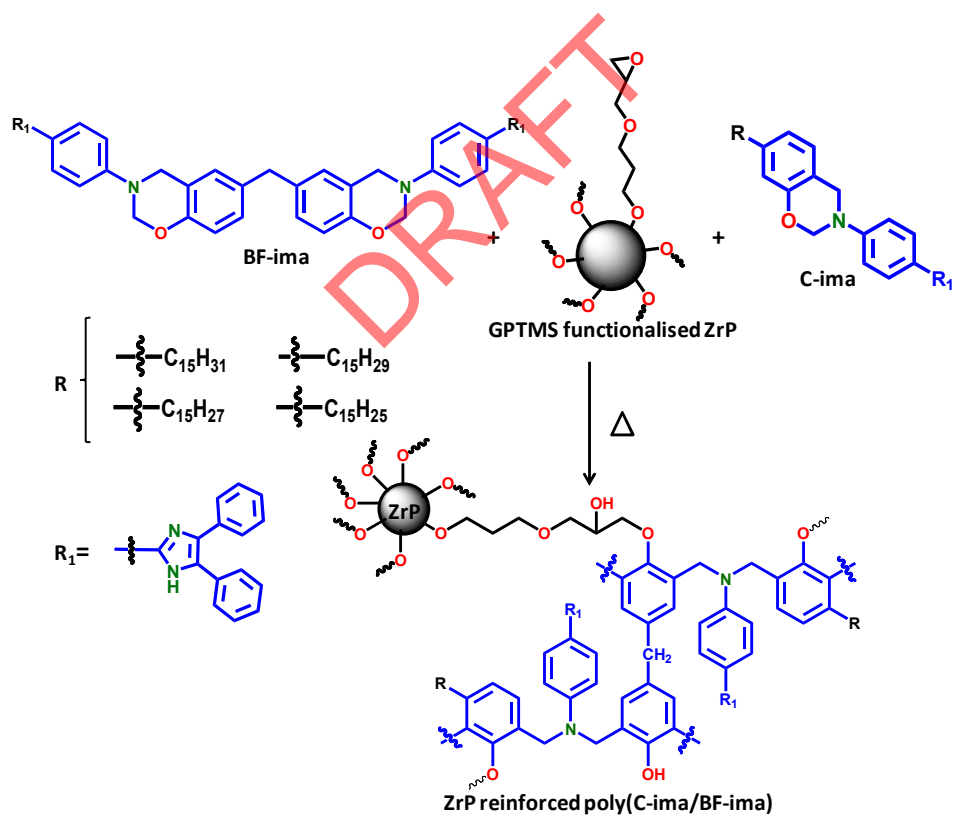
Scheme 3. Synthesis of BF-ima benzoxazine monomer



Scheme 4. Preparation of Silane Functionalization of ZrP



**Scheme 5. Synthesis of poly(C-ima/BF-ima) benzoxazines blended matrix**



**Scheme 6. Preparation of ZrP reinforced poly(C-ima/BF-ima) benzoxazines blended composites**



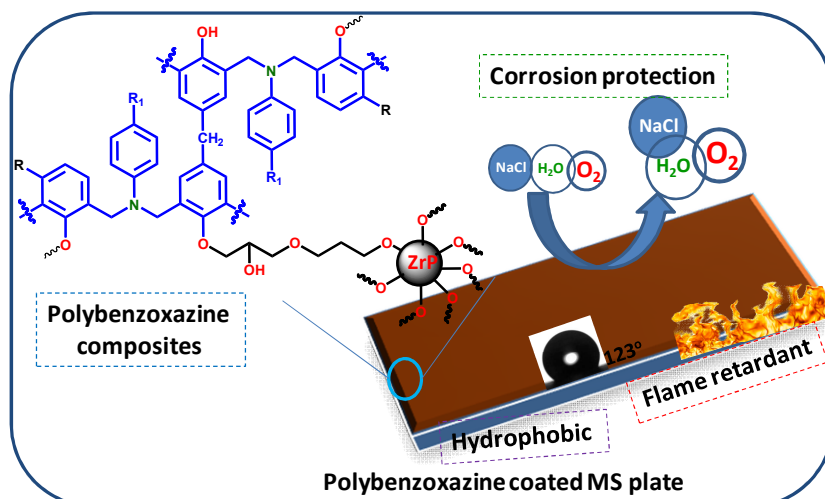


Figure 1. Benzoxazine coating on MS plate for hydrophobic, flame retardant and corrosion protection application.

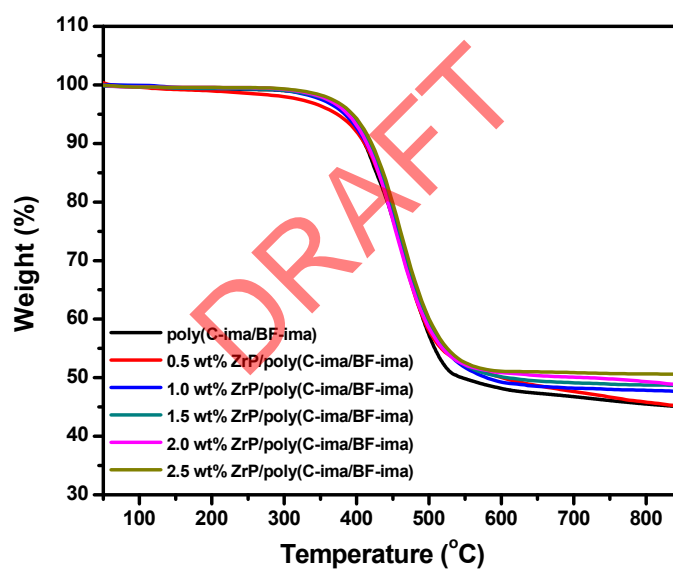
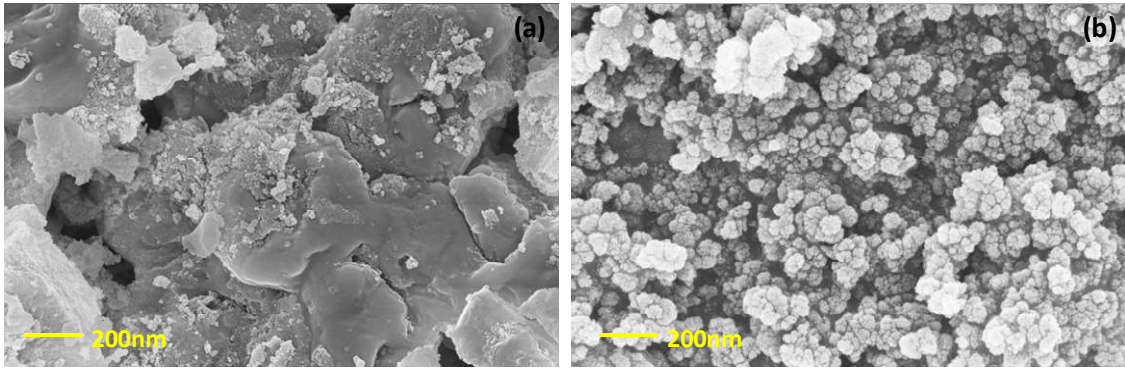
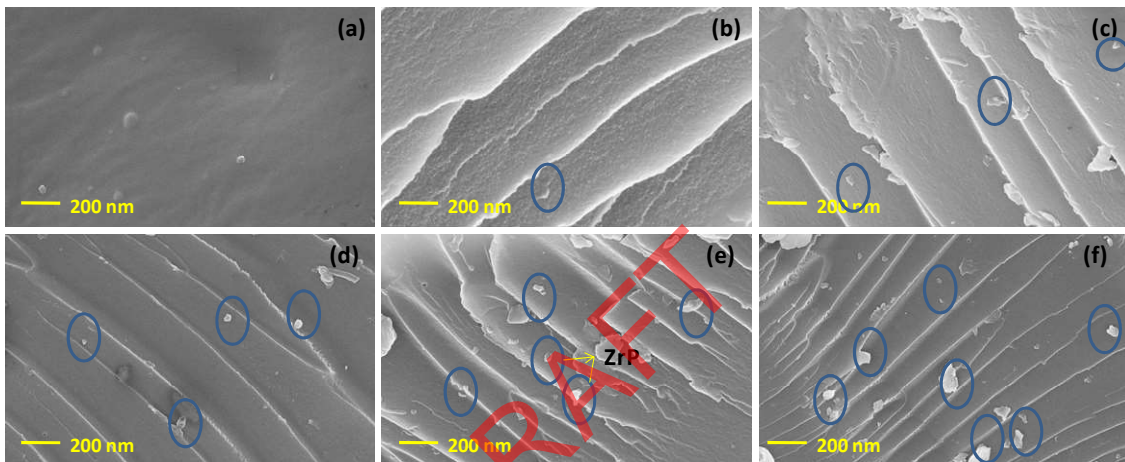


Figure 2. TGA thermogram of ZrP reinforced polybenzoxazine blended composites



**Figure 3.** SEM micrographs of (a) ZrP, (b) GPTMS functionalised ZrP.



**Figure 4.** SEM micrographs of (a) neat blend of poly(C-ima/BF-ima), (b) 0.5 wt %, (c) 1.0 wt % (d)1.5 wt%, (e) 2.0 wt % and (f) 2.5 wt % ZrP reinforced poly(C-ima/BF-ima) blended composites.

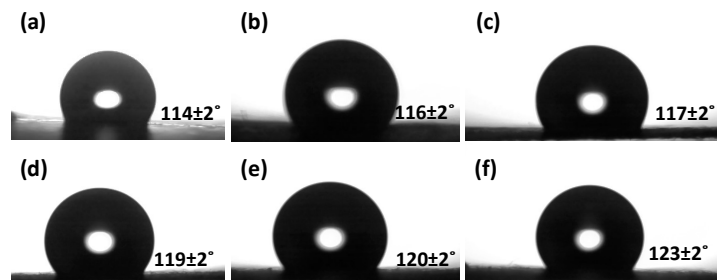


**Figure 5.** The water contact angle of (a) neat blend of poly(C-ima/BF-ima), (b) 0.5 wt %, (c) 1.0 wt % (d)1.5 wt%, (e) 2.0 wt % and (f) 2.5 wt % ZrP reinforced poly(C-ima/BF-ima) blended composites.

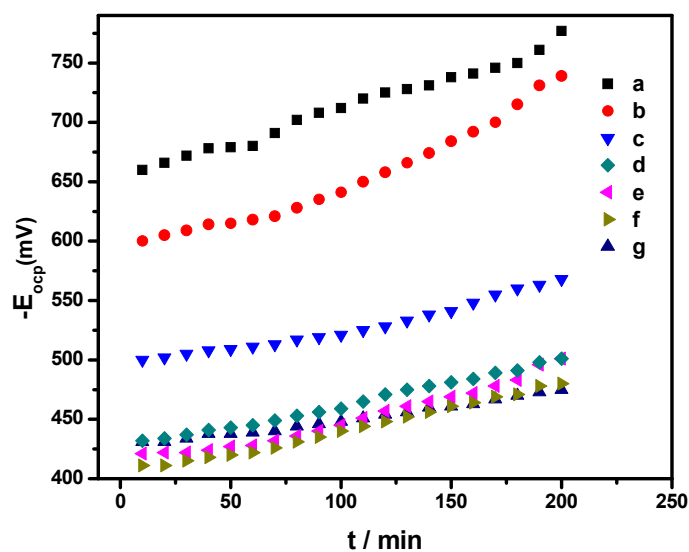


Figure 6. Plot of  $E_{ocp}$  Vs time in 3.5% of NaCl solution for (a) bare mild steel specimen (b) neat matrix, (c) 0.5 wt%, (d) 1.0 wt%, (e) 1.5 wt%, (f) 2.0 wt% and (g) 2.5 wt% ZrP reinforced poly(C-ima/BF-ima).

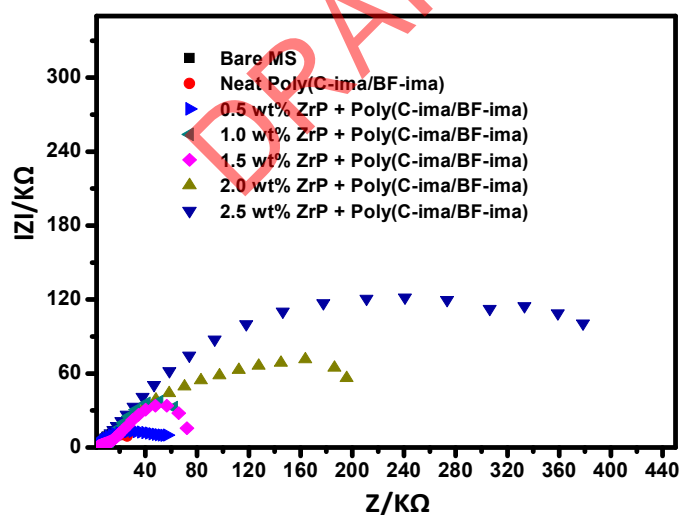


Figure 7. EIS response of bare MS and ZrP reinforced poly(C-ima/BF-ima) benzoxazine blended composites coated specimen in 3.5% NaCl solution

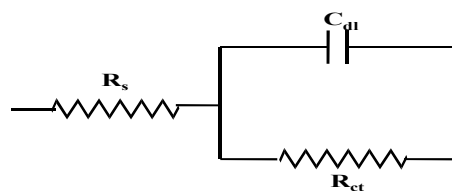


Figure 8. The equivalent circuit used for impedance analysis

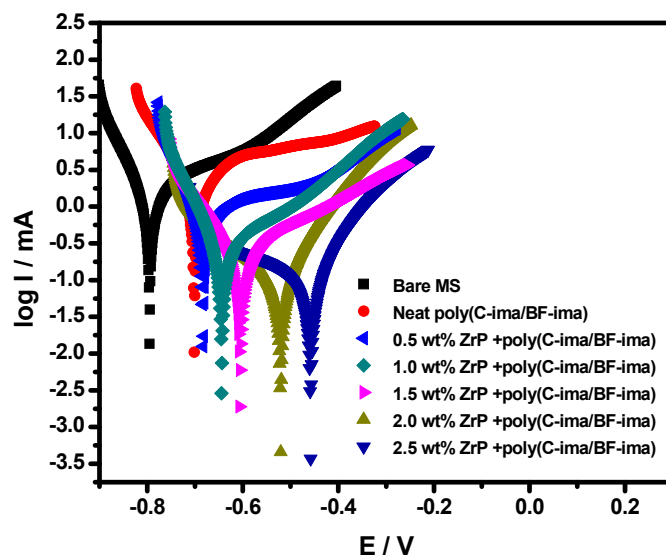


Figure 9. Tafel plots of bare MS and ZrP reinforced polymer composites coated specimens in 3.5% NaCl solution

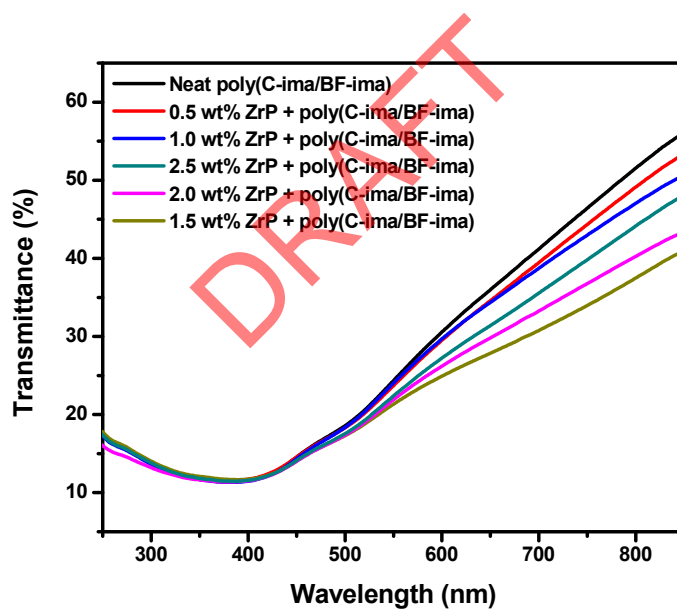


Figure 10. UV transmittance spectra of neat poly(C-ima/BF-ima) matrix and ZrP reinforced poly(C-ima/BF-ima) composites

## Tables

**Table 1. Thermal behavior of neat benzoxazines matrices**

Neat Matrices	Thermal behaviour				
	T <sub>p</sub> (°C)	10% weight loss (°C)	T <sub>max</sub> (°C)	Char yield at 850°C (%)	LOI
Poly(C-ima )	218	383	453	23	26.7
Poly(BF-ima )	202	442	491	61	41.9
Poly(50 wt% C-ima/ 50 wt% BF-ima )	202	412	468	45	35.5

**Table 2. Thermal properties and water contact angle values of ZrP reinforced polybenzoxazine blended composites**

Sample	Thermal stability				Contact angle (θ)
	10% weight loss (°C)	T <sub>d</sub> (°C)	Char yield % at 850°C	LOI	
Poly(C-ima/BF-ima)	412	468	45	35.5	114
0.5 wt% ZrP+ poly(C-ima/BF-ima)	412	468	46	35.9	116
1.0 wt% ZrP+ poly(C-ima/BF-ima)	413	470	47	36.3	117
1.5 wt% ZrP+ poly(C-ima/BF-ima)	416	470	48	36.7	119
2.0 wt% ZrP+ poly(C-ima/BF-ima)	418	471	49	37.1	120
2.5 wt% ZrP+ Poly(C-ima/BF-ima)	419	471	51	37.9	123

**Table 3. Corrosion parameters of the coated and bare mild steel specimens in 3.5 % NaCl solution calculated from potentiodynamic polarisation studies**

Samples	$R_s$ ( $\Omega \text{ cm}^2$ )	$CPE_c$		$R_c$ ( $k\Omega \text{ cm}^2$ )	$CPE_{dl}$		$R_{ct} /$ $k\Omega \text{ cm}^2$
		( $F.s^{n-1}$ )	n		( $F.s^{n-1}$ )	n	
Bare MS	6.34	$05.75 \times e^{-2}$	0.878	1.3	$11.64 \times e^{-3}$	0.727	29
Poly(C-ima/BF-ima)	07.81	$11.30 \times e^{-2}$	0.721	1.7	$02.26 \times e^{-3}$	0.739	80
0.5 wt% ZrP+ poly(C-ima/BF-ima)	02.40	$01.50 \times e^{-3}$	0.775	11.11	$01.03 \times e^{-2}$	0.781	85
1.0 wt% ZrP+ Poly(C-ima/BF-ima)	09.09	$03.40 \times e^{-4}$	0.769	28.45	$08.03 \times e^{-3}$	0.777	87
1.5 wt% ZrP+ Poly(C-ima/BF-ima)	09.23	$02.04 \times e^{-4}$	0.776	34.88	$07.90 \times e^{-4}$	0.735	88
2.0 wt% ZrP+ Poly(C-ima/BF-ima)	09.40	$15.04 \times e^{-4}$	0.775	49.22	$02.70 \times e^{-4}$	0.725	271
2.5 wt% ZrP+ Poly(C-ima/BF-ima)	10.21	$03.90 \times e^{-4}$	0.701	71.91	$02.58 \times e^{-5}$	0.721	565

**Table 4. The values of the corrosion parameters of the coated and uncoated mild steel specimens in 3.5 % NaCl solution calculated from Tafel studies**

Sample name	$E_{corr}(mV)$	$I_{corr}(\mu A)$	CR $mm \text{ year}^{-1}$	Efficiency $\eta (\%)$
Bare MS	-809	1250	0.0487	0
Poly(C-ima/BF-ima)	-701	570	0.0222	54.44
0.5 wt% ZrP+ poly(C-ima/BF-ima)	-685	207	0.0081	83.44
1.0 wt% ZrP+ Poly(C-ima/BF-ima)	-648	181	0.0071	85.52
1.5 wt% ZrP+ Poly(C-ima/BF-ima)	-607	176	0.0069	85.92
2.0 wt% ZrP+ Poly(C-ima/BF-ima)	-525	108	0.0042	91.36
2.5 wt% ZrP+ Poly(C-ima/BF-ima)	-452	101	0.0039	91.92